Eur J Pediatr (2002) 161: 26–30
DOI 10.1007/s00431-001-0852-1

ORIGINAL PAPER

Stefan A. Tschanz · Beat Haenni · Peter H. Burri

Glucocorticoid induced impairment of lung structure assessed by digital image analysis

Revised: 25 June 2001 / Revised: 29 August 2001 / Accepted: 30 August 2001 / Published online: 25 October 2001

Abstract Glucocorticoids (GC) are successfully applied in neonatology to improve lung maturation in preterm born babies. Animal studies show that GC can also impair lung development. In this investigation, we used a new approach based on digital image analysis. Microscopic images of lung parenchyma were skeletonised and the geometrical properties of the septal network characterised by analysing the 'skeletal' parameters. Inhibition of the process of alveolarisation after extensive administration of small doses of GC in newborn rats was confirmed by significant changes in the 'skeletal' parameters. The induced structural changes in the lung parenchyma were still present after 60 days in adult rats, clearly indicating a long lasting or even definitive impairment of lung development and maturation caused by GC. *Conclusion:* digital image analysis and skeletonisation proved to be a highly suited approach to assess structural changes in lung parenchyma.

Keywords Digital image analysis · Glucocorticoids · Lung · Microscopy · Morphometry

Abbreviations *allseg* all segments · *Dexa* dexamethasone · *endseg* end segments · *ep* end points · *GC* glucocorticoid · *interseg* internodal segments · *lm* mean linear intercept · *np* nodal points

Introduction

Dexamethasone (Dexa), a potent glucocorticosteroid (GC), is often used in neonatology, mainly with the aim of intrauterine enhancement of surfactant production in imminent preterm births. GCs are also used as a treatment in chronic lung disease or bronchopulmonary dysplasia after neonatal respiratory distress syndrome, often combined with assisted ventilation and oxygen supply. The application of GCs is still controversial: There are doubts about the long-term benefit of this treatment and there is strong evidence from animal experiments that GCs impair lung maturation [8, 9, 11,16].

The delicate architecture of the lung parenchyma is organised to meet the oxygen requirements of the organism. Oxygen uptake relies upon the size of diffusion surface area and on the thickness of the diffusion barrier between air and blood. Disturbances of the structure of the inter-airspace walls of the parenchyma will usually lead to a decrease in available surface area and/or to an increase in diffusion barrier thickness. The lung is particularly susceptible to perinatal influences because development and maturation take place very late in gestation and even last until after birth. A major proportion of all neonatal complications relates to problems with the respiratory tract and is often associated with lung immaturity.

In a previous publication [16] we investigated the lungs of rats treated post-natally with minute doses of Dexa for 2 weeks in the phase when most alveoli are formed by septation. The morphological findings revealed a drastic impairment in post-natal lung maturation with a decreased rate of septation, resulting in a decreased number of alveoli. Some of the morphological findings were also confirmed by morphometric analysis. The obvious widening of air spaces, persisting until adolescence, were constantly detectable by eye but the standard morphometric parameters like surface area density and volumetric data did not significantly confirm these findings (Fig.1). We intended therefore to develop a technique allowing to quantitatively assess these apparent differences in parenchymal air space geometry. The new approach relied on digital image analysis creating a "skeleton" of the lung parenchymal architecture, followed by automated measurements of the 'skeletal' components.

S.A. Tschanz (✉) · B. Haenni · P.H. Burri
Institute of Anatomy, University of Berne,
Buehlstrasse 26, 3000 Berne 9, Switzerland
E-mail: tschanz@ana.unibe.ch
Tel.: +41-31-6318478
Fax: +41-31-6313410

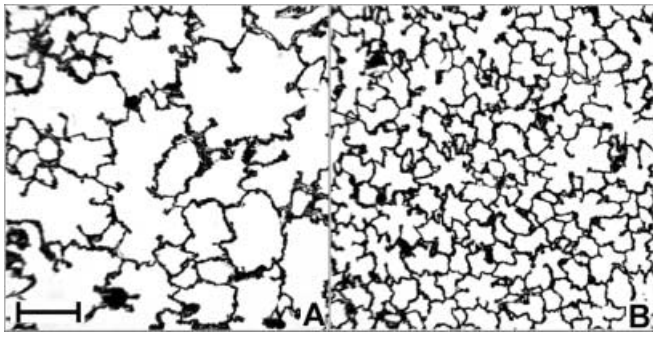

Fig. 1 Light microscopic photomicrograph of lung parenchyma in 60 day-old rats. **A** Animals treated with GCs during early childhood. **B** Control animals. Bar = 100μm. (Haemalum-Eosin)

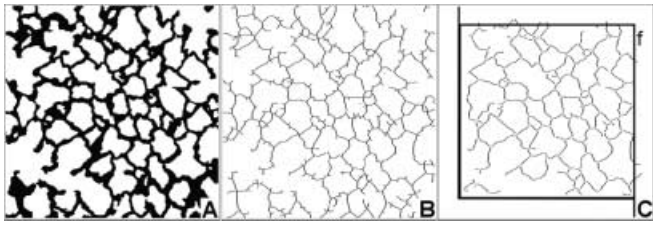

Fig. 2 Series of images showing the main image processing steps to obtain 'skeletons'. **A** Binarised image by a threshold level assigning all septal tissue to blue and air spaces to yellow. **B** Same image after skeletonising. **C** 'Skeleton' after correction and segmentation. Segments, touching the border and not lying within the counting frame (*f*) were removed

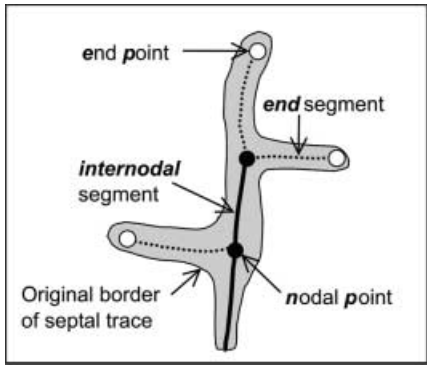

Fig. 3 Diagram showing the assignment of segments to the septal traces

Materials and methods

This work is based on animal samples from a previous experiment [16] to which we refer for details about animal care and drug administration. In summary, male rats of the SIV Z-50 strain were housed in groups of eight animals per litter with their mothers and from 30 days on in single cages. Day 1 was the 1st day after birth. From days 2 to 15 after birth they received 50 μl of Dexa (Decadron, kindly provided by Merck, Sharp and Dohme; 1 ml of Decadron contains 4 mg of dexamethasone phosphate) diluted 1:2000 with isotonic saline (0.1 μg dexamethasone phosphate per animal and day) by subcutaneous injection between 9 and 10 a.m. Age matched control animals received a similar dose of isotonic saline.

Lung fixation and tissue processing

On days 36, 44 and 60, four animals per group and day were deeply anaesthetised and their lungs fixed according to standard techniques [5], i.e. the lungs were fixed by intratracheal instillation of a 2.5% buffered glutaraldehyde solution applying a 20 cm H_2O pressure head. Following removal of the chest organs and dissection of the lung, the right middle lobe was embedded in toto in methacrylate for light microscopy. "Serial" step sections, 2 μm in thickness and taken every 180 μm, were cut and stained with fuchsine. This method produced a homogeneous high contrast tissue staining favourable for digital image analysis. From this series, three to four equidistantly spaced sections were randomly taken for light microscopic image analysis.

Image sampling

The sections of lung parenchyma were viewed on a Leica DM RB light microscope equipped with a motorised Maerzheuser XY stage. Microscope fields were observed with a ×10 objective and captured by a Sony DX 930 3-chip video camera. For every animal, 30 images were taken according to a systematic random sampling by moving the specimen slide with the programmable motor stage.

Image processing

All image processing and analysis steps were performed on a PC based imaging system (Visilog, Noesis SA, France), including a Matrox 1280 (Matrox Ltd., Canada) frame grabber board. Image processing and analysis ran automatically interrupted only by user interactions allowing image control. A description of the digital image analysis as well as a detailed discussion of this approach and its critical stereological implications are presented in a separate publication [15]. In summary, the video signals were digitised as eight bit grey level images in a square field of view of 512×512 pixels corresponding to a side length of 1070 μm on the specimen. Image parts not belonging to the parenchyma (e.g. bronchi, large vessels, and tissue boundaries) were marked and excluded manually and subsequently not analysed. The images were corrected for illumination inhomogeneities and segmented into binary images by an adaptive threshold filtering. In the resulting images, a positive pixel signal corresponded to the tissue and zero values to the air spaces (background) (Fig.2). The images were processed with a skeletonising algorithm where the septal profiles were eroded from both sides until convergence of the erosion fronts was reached (Fig.2). The resulting line network consisted of internodal line segments (interseg) between two connecting points, called nodal points, (np) and end segments (endseg) between a nodal point and a free ending at a so-called end point (ep) (Fig.3). The skeleton images were checked and corrected for artifacts. Prior to measuring, they were split into unconnected segments by removing all np (Fig.2). In order to avoid border artifacts, all measurements were performed within a counting frame (Fig.2) respecting the forbidden line rule established by Gundersen [7]. The number of ep and np, of internodal and endseg per field was computed. The length of every segment was calculated and collected in a table.

Characterisation of the skeletal network and thus of the lung parenchyma was achieved by the statistical analysis of the following skeleton parameters: numerical density of ep and np per mm^2 (N ep/mm^2, N np/mm^2), numerical density of endseg and internodal segments and of allseg per mm^2 (N endseg/mm^2, N interseg/mm^2, N allseg/mm^2), length density of each segment category and of allseg per mm^2 (L interseg/mm^2, L endseg/mm^2, L allseg/mm^2), mean individual segment length in each category in μm (l_{mean} interseg, l_{mean} endseg), and maximal individual segment length in each category in μm (l_{max} interseg, l_{max} endseg).

Statistics

Values presented are means of four animals per group and day ($n=4$). Statistical analysis was performed with a two-tailed Student's t-test. Significance level was reached where $P<0.05$.

Results

The analysis of the lung parenchyma skeletons yielded drastic differences between rats treated post-natally with Dexa compared to age matched controls at all days of observation (days 36, 44, 60). Values are listed in Table1 and Table2.

The difference in the average numerical density of allsegs (N allseg/mm^2) between groups was pronounced. On each day, the number of segments in the Dexa group was inferior by about one third (34%–39%) compared to controls ($P<0.05$). Likewise the mean length density of segments per field (L allseg/mm^2) was reduced by over 25% in the Dexa group ($P<0.05$) on all days. These changes were mainly based on differences in the internodal parameters, N interseg/mm^2 and L interseg/mm^2, which with 65%–75%, represented the major part of all segments. The values for endseg, N endseg/mm^2 and L endseg/mm^2, showed the same trend but the decrease in the Dexa group reached significance only for day 44. The extensive decrease in numerical interseg density (N interseg/mm^2) in all Dexa animals in combination with the more stable N endseg/mm^2 values resulted in a shift of the ratio end to internodal segments (N end/N interseg) in favour of the endseg (Table1) ($P<0.01$).

The parameters of ep and np were conformable with the segment data. The mean numerical density of np, N np/mm^2, was decreased on all days in the Dexa group. The density decrease of ep, N ep/mm^2, was less important, but nevertheless, reached significance on day 44 (–22%, $P<0.02$). The proportion of np and ep was shifted towards ep, which implies a lesser impairment of septal tips in the Dexa group.

The pattern of individual segment lengths of both segment categories also varied within the animal groups. Mean individual length of interseg (l_{mean} interseg) was significantly increased in the Dexa group on all days, i.e. by 31%, 28% and 18% on days 36, 44 and 60, respectively. The maximal length of interseg in the Dexa group, l_{max} interseg, was also increased on all days. The

Table 1 Numerical density (N) of points and segments. Values are means of groups of ($n=4$) animals. (*SEM* standard error of the mean)

		N nodal points (Nnp/mm^2)		N end points (Nep/mm^2)		N internodal segments (Ninterseg/mm^2)		N end seg (Nendseg/mm^2)		Ratio of end to internodal segment density (Nendseg/Ninterseg)		N allseg (Nallseg/mm^2)	
		mm^{-2}	SEM	mm^{-2}	SEM	mm^{-2}	SEM	mm^{-2}	SEM	Ratio	SEM	mm^{-2}	SEM
Day 36	Control	559.4	28.5	214.5	6.7	658.8	35.0	196.4	4.2	0.299	0.012	855.3	38.5
	Dexa	357.8	59.3*	180.8	24.8	395.2	63.9*	165.9	23.9	0.426	0.023**	561.1	87.3*
Day 44	Control	558.9	26.9	234.8	10.4	657.4	35.6	211.7	5.0	0.325	0.020	869.1	36.0
	Dexa	318.0	38.6**	177.0	24.6	354.5	42.0**	162.9	18.2*	0.462	0.016**	517.4	59.5**
Day 60	Control	499.4	48.3	201.9	11.9	583.7	62.3	188.8	9.3	0.332	0.029	772.5	69.7
	Dexa	301.5	18.1**	178.8	21.5	325.9	21.1**	165.8	5.3	0.512	0.029**	491.6	26.0**

*$P<0.05$
**$P<0.01$

Table 2 Segment lengths. Values are means of groups of ($n=4$) animals.(*SEM* standard error of the mean)

		Length density of internodal segments (L interseg/mm^2)		Mean individual length of internodal segment (l_{mean} interseg)		Max individual length of internodal segment (l_{max} interseg)		Length density of end segments (L endseg/mm^2)		Mean individual length of end segments (l_{mean} endseg)		Max individual length of end segments (l_{max} endseg)		Length density of all segments (L allseg/mm^2)	
		mm/mm^2	SEM	µm	SEM	µm	SEM	mm/mm^2	SEM	µm	SEM	µm	SEM	mm/mm^2	SEM
Day 36	Control	20.8	0.7	31.9	0.7	151.7	2.7	5.34	0.15	27.15	0.28	113.7	3.2	26.14	0.80
	Dexa	15.6	1.2*	41.9	3.4	198.6	13.4*	4.53	0.45	28.09	1.82	139.1	6.3*	20.14	1.54*
Day 44	Control	21.1	0.8	32.5	0.6	147.8	3.1	5.97	0.19	28.24	0.93	117.8	5.1	27.09	0.66
	Dexa	14.1	0.9**	41.5	3.0*	188.7	12.3*	4.74	0.32*	29.90	1.66	153.5	11.6*	18.85	1.19**
Day 60	Control	20.8	1.5	36.5	1.7	166.6	8.5	5.16	0.25	27.36	0.22	117.1	5.3	25.91	1.68
	Dexa	13.7	0.7**	43.1	1.1*	198.5	4.6*	4.78	0.11	28.98	0.35**	158.0	2.9**	18.46	0.73**

*$P>0.05$
**$P<0.01$

endseg showed only a slight increase in the mean individual segment length, l_{mean} endseg in the Dexa group, by 3%, 6%, and 6% on days 36, 44 and 60, respectively. The latter difference on day 60 was significant. The maximal length of the endseg, l_{max} endseg, was increased in the Dexa group on all days.

Discussion

Some effects of GCs on lung development and maturation have already been described 40 years ago. In the 1960s, they were identified as potent accelerators of the maturation of type 2 lung epithelial cells with stimulation of the surfactant production [2]. Later GCs were also used in the therapy of mainly preterm born babies with respiratory distress syndrome and at risk of suffering from bronchopulmonary dysplasia, recently renamed chronic lung disease. The inhibitory influence of GCs on structural lung development and maturation is also well established. Since the first reports on the suppression of post-natal alveolarisation by these drugs in the rat by Massaro et al. [8,9], further studies confirmed the original findings [1, 10, 11,14]. In a recent morphological and quantitative study, we proposed that alveolarisation was prevented because the GCs accelerated lung maturation in terms of inducing microvascular maturation at a precocious stage [16]. Since the formation of a new alveolar "daughter" septum requires a "mother" septum containing two capillary layers [4], the precocious microvascular maturation with reduction of the double layered septa into single layered ones [6] depresses indirectly the formation of new septa, i.e. of new alveoli. In our experiment, the GCs were given in minute doses from day 2 to day 15 during the critical phase of alveolarisation in the rat, when the bulk of the alveoli are formed (bulk alveolarisation) [3]. After withdrawal of drug treatment we had observed a recovery phenomenon involving a step back in maturation with reappearance of double capillary layers and regrowth of new septal crests. Despite this effort to compensate for the failure of bulk alveolarisation, the lungs from the Dexa group still appeared "emphysematous" on days 36, 44 and 60. The morphometric measurements of a combined light microscopic and electron microscopic analysis of Dexa group and control lungs (surface area of air spaces, mean linear intercepts) did not support to the same extent the marked visual impression to any significant difference. Indeed, only few differences in a large number of data reached significance, the best parameter being the mean linear intercept (lm). It was significantly increased in our study only on day 44, while Thibeault and coworkers (1993) found lm elevated on day 60 [13]. The differences in alveolar surface density, however, did generally not allow a statistically safe statement.

This problem of "incongruence" between visual impression and morphometric data in the alveolarisation process has been noticed by others (D. Massaro, personal communication). It may reside partly in the combination of light microscopic and electron microscopic measurements: at the electron microscopic level, where the surface area measurements are done, an increase in roughness of the air blood barrier could account for a higher surface area density detection and compensate for a parallel decrease in parenchymal complexity. We therefore developed an approach relying directly on the visual impression provided by two-dimensional images. Based on digital image processing and analysis, the geometrical properties of parenchymal tissue and air spaces were parameterised by analysing the 'skeletons' derived from the light microscopic parenchymal lung sections. This simplified representation of the septal meshwork contained the information about the geometry of tissue and air spaces. After reanalysing the same lung sections of the previous study, the results obtained clearly and significantly expressed the changes in the geometry of lung parenchyma in the Dexa group versus controls.

In the Dexa group, a 34%, 40% and 35% decrease in the total number of skeleton segments per mm^2 was observed on days 36, 44 and 60, respectively. This decrease consisted mainly in a reduction of internodal segments (40%, 44% and 46%) and accordingly in a decrease in np, connecting them. The mean individual length of internodal segments, however, was much higher in the Dexa group and represented very well the distended aspect of these lungs. In fact, the increased mean individual length of interseg stood for septal traces having fewer branchings, i.e. less connections to neighbouring septa. We could conclude that in the Dexa group there were less neighbouring alveoli per area. On the other hand, the decrease in mean length of interseg in the controls combined with an increase in the number density of these segments and of np indicated that more alveoli were attached to each other per area. It is not possible to directly infer to alveolar number from these data, but these skeleton parameters are in close relation to the alveolar density. Despite the longer internodal segments in the Dexa group, the total length density of segments, L allseg/mm^2 (i.e. the sum of the length of interseg and endseg per mm^2) was significantly decreased in the Dexa group due to an overproportional decrease in the number density of segments. This fact supported strongly a functional impairment of lung parenchyma in the Dexa group, since L allseg/mm^2 is proportional to the surface area density of air spaces [15].

Interestingly the decrease in ep density was smaller than that of np in the Dexa group (day 36: –17% in ep versus –37% in np; day 44: –22% versus –43% and day 60: –6% versus –36%). Conclusively the length density of alveolar mouths was less decreased in the Dexa group than the length density of the septal connecting lines. Contrary to the marked increase in mean interseg length in the Dexa group, the mean endseg length was barely changed (+3%, +6% and +6% increase in the Dexa group). If we assume, based on the visual impression and the skeletal data, that the air spaces were generally wider

in the Dexa group, the practically unaffected mean endseg length signals a widening of ductal air spaces.

The stereological implications of the interpretations of the skeleton into the three-dimensional space have been extensively discussed elsewhere [15]. The skeleton corresponds to the traces of the median planes of the septa in a section. It can be decomposed into three categories of segments defined by internodal and eps (see Methods). While the intersegs are difficult to attribute to defined 3-dimensional structures, their number density, their length density and the number density of internodal points are a reflection of the complexity of the lung parenchyma. The number of eps, however, represents a direct measurement of the line network forming the alveolar mouths and the total length density of all skeleton segments is a good estimate of the alveolar surface area density [15]. The present skeletonisation results confirm on a quantitative basis our previous suggestion that alveolarisation is depressed by long-term administration GCs even with a minute dose of Dexa. The findings are in agreement with other previous reports [9,11]. The full complexity of the parenchymal network was not attained after inhibition of septation during the period of normal bulk alveolarisation, despite an additional "second-round" process of alveolarisation after the end of hormone treatment [16].

We are aware that the new quantitative approach lacks partially an interpretation in the third dimension, however, the counting of alveoli and alveolar ducts was and remains a tricky or even inaccurate procedure. The characterisation of an alveolus as a countable entity on a section is not practicable. Unbiased estimators of particle number in space like the disector [12] must also fail because of the lack of spatial definition of an alveolus. We therefore believe that the description of parenchymal geometry by variables taken from two-dimensional skeletons represents a valuable and sensitive alternative to assess changes in parenchymal architecture. Furthermore, it has the advantage of being lenient on manpower.

Acknowledgements The authors wish to thank Mrs Marianne Hofstetter, Mrs Elisabeth de Peyer, Mr Christoph Lehmann, Mr Karl Babl and Mr Hans-Juerg Keller for their technical assistance. This work was supported by Grant Nos. 31-45831.95 and 31-55895.98 from the Swiss National Science Foundation.

References

1. Blanco LN, Frank L (1993) The formation of alveoli in rat lung during the third and fourth postnatal weeks: effect of hyperoxia, dexamethasone, and desferroxamine. Pediatr Res 34: 334–340
2. Buckingham S, Avery ME (1962) Time of appearance of lung surfactant in the foetal mouse. Nature 193: 688–689
3. Burri PH (1974) The postnatal growth of the rat lung. III. Morphology. Anat Rec 180: 77–98
4. Burri PH (1997) Structural aspects of prenatal and postnatal development and growth of the lung. In: McDonald J (ed) Lung growth and development. Marcel Dekker, New York pp 1–35
5. Burri PH, Dbaly J, Weibel ER (1974) The postnatal growth of the rat lung. I. Morphometry. Anat Rec 178: 711–730
6. Caduff JH, Fischer LC, Burri PH (1986) Scanning electron microscopic study of the developing microvasculature in the postnatal rat lung. Anat Rec 216: 154–164
7. Gundersen HJG (1977) Notes on the estimation of the numerical density of arbitrary profiles: the edge effect. J Microsc 111: 219–223
8. Massaro D, Massaro GD (1986) Dexamethasone accelerates postnatal alveolar wall thinning and alters wall composition. Am J Physiol 251: R218–R224
9. Massaro D, Teich N, Maxwell S, Massaro GD, Whitney P (1985) Postnatal development of alveoli. Regulation and evidence for a critical period in rats. J Clin Invest 76: 1297–1305
10. Navarro HA, Kudlacz EM, Eylers JP, Slotkin TA (1989) Prenatal dexamethasone administration disrupts the pattern of cellular development in rat lung. Teratology 40: 433–438
11. Sahebjami H, Domino M (1989) Effects of postnatal dexamethasone treatment on development of alveoli in adult rats. Exp Lung Res 15: 961–973
12. Sterio DC (1984) The unbiased estimation of number and sizes of arbitrary particles using the disector. J Microsc 134: 127–136
13. Thibeault DW, Heimes B, Rezaiekhaligh M, Mabry S (1993) Chronic modifications of lung and heart development in glucocorticoid-treated newborn rats exposed to hyperoxia or room air. Pediatr Pulmonol 16: 81–88
14. Torday JS, Zinman HM, Nielsen HC (1986) Glucocorticoid regulation of DNA, protein and surfactant phospholipid in developing lung. Temporal relationship between growth and differentiation. Dev Pharmacol Ther 9: 125–131
15. Tschanz SA, Burri PH (2001) A new approach to detect structural differences in lung parenchyma using digital image analysis. Exp Lung Res (in press)
16. Tschanz SA, Damke BM, Burri PH (1995) Influence of postnatally administered glucocorticoids on rat lung growth. Biol Neonate 68: 229–245